

RANGE IDENTIFICATION FOR A PERSPECTIVE DYNAMIC SYSTEM WITH A SINGLE HOMOGENEOUS OBSERVATION

LILI MA*, YANGQUAN CHEN*, KEVIN L. MOORE**

* Center for Self-Organizing and Intelligent Systems (CSOIS)
Department of Electrical and Computer Engineering, 4160 Old Main Hill
Utah State University (USU), Logan, UT 84322–4160, USA
e-mail: lilima@cc.usu.edu, yqchen@ece.usu.edu

** Research and Technology Development Center
Johns Hopkins University Applied Physics Laboratory
M/S 2–236 11100, Johns Hopkins Road Laurel, MD 20723-6099, USA
e-mail: kevin.moore@jhuapl.edu

Perspective problems arise in machine vision when using a camera to observe the scene. Essential problems include the identification of unknown states and/or unknown parameters from perspective observations. Range identification is used to estimate the states/positions of a moving object with known motion parameters. Range estimation has been discussed in the literature using nonlinear observers with full homogeneous observations derived from the image plane. In this paper, the same range identification problem is discussed with a single homogeneous observation using nonlinear observers. Our simulation results verify the convergence of the observers when their observability conditions are satisfied.

Keywords: range identification, perspective dynamic systems, nonlinear observer

1. Introduction

In 3D motion estimation from image sequences, there are basically two sub-categories of identification problems. One category is to estimate the parameters of the motion dynamics of a moving object. The other is to recover the depth information assuming that the motion parameters are already known. The solutions to the first sub-category of problems can be resolved, to the extent possible, via algorithms such as nonlinear optimization formulations (Cho *et al.*, 2001), linear least squares/total least squares approximations (Papadimitriou *et al.*, 2000), the application of epipolar constraints (Soatto *et al.*, 1996), and nonlinear observers (Chiuso *et al.*, 2002; Ghosh *et al.*, 1994; Jankovic and Ghosh, 1995). The second sub-category of problems, which is the main focus of this paper and is referred to as the range identification problem hereafter, can be solved by nonlinear observers applied to perspective dynamic systems (PDS), which is a class of linear systems with homogeneous observation functions.

With a stationary camera observing a moving object, we assume that the object follows an affine motion described by the following system of ordinary differential equations:

$$\begin{bmatrix} \dot{X}(t) \\ \dot{Y}(t) \\ \dot{Z}(t) \end{bmatrix} = \begin{bmatrix} a_{11} & a_{12} & a_{13} \\ a_{21} & a_{22} & a_{23} \\ a_{31} & a_{32} & a_{33} \end{bmatrix} \begin{bmatrix} X(t) \\ Y(t) \\ Z(t) \end{bmatrix} + \begin{bmatrix} b_1 \\ b_2 \\ b_3 \end{bmatrix}. \quad (1)$$

Then, a typical PDS will consist of the above linear dynamic system with the following homogeneous output observations:

$$y_1(t) = X(t)/Z(t), \quad y_2(t) = Y(t)/Z(t). \quad (2)$$

The range identification problem can be described formally in the framework of PDSs. That is, assuming that the motion parameters $a_{i,j}$ and b_i for $i, j = 1, 2, 3$ are known, the range estimation problem is to estimate the position of an object with an unknown initial condition from observations on the imaging surface (Chen and Kano, 2002; Dixon *et al.*, 2003; Jankovic and Ghosh, 1995).

Let

$$\begin{aligned} y(t) &= [y_1(t), y_2(t), y_3(t)]^T \\ &= [X(t)/Z(t), Y(t)/Z(t), 1/Z(t)]^T. \end{aligned} \quad (3)$$

The derivative of $y(t)$ is

$$\begin{cases} \dot{y}_1(t) = a_{13} + (a_{11} - a_{33})y_1 + a_{12}y_2 - a_{31}y_1^2 \\ \quad - a_{32}y_1y_2 + (b_1 - b_3y_1)y_3, \\ \dot{y}_2(t) = a_{23} + a_{21}y_1 + (a_{22} - a_{33})y_2 - a_{31}y_1y_2 \\ \quad - a_{32}y_2^2 + (b_2 - b_3y_2)y_3, \\ \dot{y}_3(t) = -(a_{31}y_1 + a_{32}y_2 + a_{33})y_3 - b_3y_3^2. \end{cases} \quad (4)$$

It is based on the above equivalent nonlinear dynamic system that nonlinear observers have been designed/applied to estimate $y_3(t)$ from $y_1(t)$ and $y_2(t)$.

Assuming that both $y_1(t)$ and $y_2(t)$ are available, several observers have been designed/applied to the nonlinear dynamics in (4), including the following:

- The Identifier-Based Observer (IBO) proposed in (Jankovic and Ghosh, 1995), which is motivated by adaptive control theory.
- The state observer (referred to as the SMO due to its employment of a sliding mode method) in (Chen and Kano, 2002), which is a combination of the sliding mode control method, the adaptive method, and discontinuous observer techniques.
- The Range Identification Observer (RIO) in (Dixon et al., 2003), which facilitates a Lyapunov-based analysis.
- The Linear Approximation-based Observer (LAO) in (Ma, 2004), which is motivated by the linear approximation idea proposed in (Hernandez et al., 2003; Tomas-Rodriguez and Banks, 2003).

In this paper, we consider the range identification problem with a single homogeneous observation. That is, we consider the problem when either $y_1(t)$ or $y_2(t)$ is known, instead of both of them. We show that with reduced information, the range identification task can be achieved, but in a less appealing manner.

The paper is organized as follows: Section 2 gives motivations to study the single observation case. In Section 3, the range identification problem with a single observation is carried out. Section 4 presents our simulation results and comparisons between the cases when $y_1(t)$ and $(y_1(t), y_2(t))$ are available. Finally, Section 5 concludes the paper.

2. Motivation

The existing vision devices typically use a photographic camera or a video camera, in conjunction with an off-the-shelf lens, where a 3D point is projected onto a plane perpendicular to the camera's optical axis. Normally we assume a pinhole camera (perspective) model. This camera-type projection is a special case of a more general planar imaging surface as shown in Fig. 1, where the plane is described by its normal vector $\vec{n} = [n_1, n_2, n_3]^T$ and a point on the plane, which is assumed to be $[0, 0, 1]$ without loss of generality.

For any point $[X_p, Y_p, Z_p]^T$ on this plane, where the subscript p denotes the projection, we have

$$n_1 X_p + n_2 Y_p + n_3 (Z_p - 1) = 0, \quad (5)$$

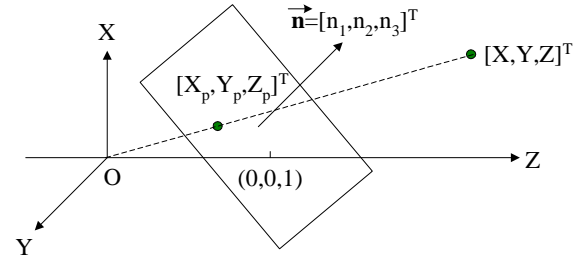


Fig. 1. A general planar imaging surface passing through $[0, 0, 1]$ with normal vector $\vec{n} = [n_1, n_2, n_3]^T$.

where we further assume that $n_3 \neq 0$ to emphasize that the observations are facing toward the Z axis. Since the projection of a 3D point $[X, Y, Z]^T$ can only be observed up to a homogeneous line as

$$X_p = Z_p X/Z, \quad Y_p = Z_p Y/Z, \quad (6)$$

from Eqns. (5) and (6), we have

$$X_p = n_3 X/p, \quad Y_p = n_3 Y/p, \quad Z_p = n_3 Z/p, \quad (7)$$

with $p \triangleq n_1 X + n_2 Y + n_3 Z$.

Define $y_g = [y_{g1}, y_{g2}, y_{g3}, y_{g4}]^T$ as

$$y_{g1} = X/p, \quad y_{g2} = Y/p, \quad y_{g3} = Z/p, \quad y_{g4} = 1/p. \quad (8)$$

The range identification of a PDS with the general planar imaging surface shown in Fig. 1 amounts to estimating y_{g4} using (y_{g1}, y_{g2}, y_{g3}) . For a conventional camera, $n_1 = n_2 = 0$, $n_3 = 1$, and this equation reduces to

$$y_{g1} = X/Z, \quad y_{g2} = Y/Z, \quad y_{g3} = 1, \quad y_{g4} = 1/Z. \quad (9)$$

Consider a more special situation, as shown in Fig. 2, when an object is moving on a plane P_1OP_2 , whose projection on the image plane is a line p_1p_2 that has either a constant $y_1(t)$ or a constant $y_2(t)$. If $y_2(t)$ is a constant, $\dot{y}_2 = 0$. Then the range identification problem is to identify $y_2(t)$ and $y_3(t)$ using $y_1(t)$.¹ The above discussion serves as another motivation for investigating the range identification problem for a PDS with a single homogeneous observation. In the following sections, $y_2(t)$ will be treated as unavailable, not necessarily as a constant.

The results presented in this work show that with reduced information, the range identification task can be performed, but in a less appealing manner. It can be further concluded that more general 3D imaging surfaces, such as the general plane shown in Fig. 1, a sphere or an ellipsoid, can be more desirable as far as range identification is concerned, since they can provide additional

¹ The case of estimating $y_1(t)$ and $y_3(t)$ from $y_2(t)$ is similar.

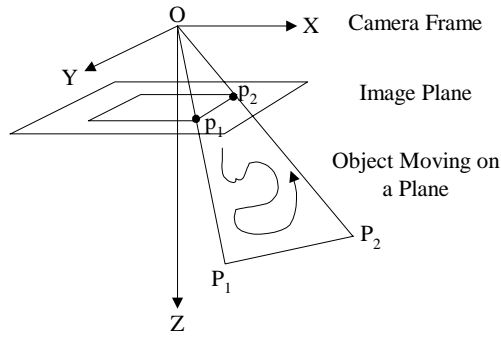


Fig. 2. Illustration of a PDS with a single observation function.

homogeneous output(s), instead of $Z = 1$ as in the case of a camera.

3. Nonlinear Observers for PDS with a Single Homogeneous Observation

In the case of a single homogeneous observation using only $y_1(t)$, the range identification task can be solved by a direct application of an IBO since the IBO observer is designed for a class of nonlinear systems in the form of (10) below. Further, based on a resemblance in the constructions of the IBO and the SMO for the case of fully homogeneous observations (with both $y_1(t)$ and $y_2(t)$), a modified SMO is used for the single observation case.

Applying the idea of constructing an RIO to the case with a single observation is not as straightforward (it might not be as appropriate either) as extending the idea of the IBO and the SMO. In an RIO, assuming that y_1 and y_2 are both available, \hat{f}_1 and \hat{f}_2 are first estimated to approximate $f_1 = (b_1 - b_3 y_1) y_3$ and $f_2 = (b_1 - b_3 y_2) y_3$, respectively. Then, the estimate of y_3 , denoted by \hat{y}_3 , is computed by (Dixon *et al.*, 2003):

$$\hat{y}_3^2 = \frac{\hat{f}_1^2 + \hat{f}_2^2}{(b_1 - b_3 y_1)^2 + (b_2 - b_3 y_2)^2}.$$

Since \hat{f}_1 and \hat{f}_2 are estimated independently of each other, we can let

$$\hat{y}_3^2 = \frac{\hat{f}_1^2}{(b_1 - b_3 y_1)^2}$$

for the single case when only y_1 is available. However, estimating y_2 from y_1 and \hat{y}_3 might not be straightforward. Further, it is obvious that when the denominators in the above two equations are small, the estimation errors of y_3 and possibly y_2 can be too conservative. Due to the above reasons, extending the idea of the RIO to a single case is not further pursued.

3.1. Direct Application of an IBO

Range identification with a single homogeneous observation can be solved by a direct application of the IBO observer, which has been applied to estimate $y_3(t)$ when both $y_1(t)$ and $y_2(t)$ are available (Jankovic and Ghosh, 1995). Consider the following class of nonlinear systems:

$$\begin{cases} \dot{\mathbf{x}}_1 = w^T(\mathbf{x}_1, \mathbf{u})\mathbf{x}_2 + \phi(\mathbf{x}_1, \mathbf{u}), \\ \dot{\mathbf{x}}_2 = g(\mathbf{x}_1, \mathbf{x}_2, \mathbf{u}), \\ \mathbf{y} = \mathbf{x}_1, \end{cases} \quad (10)$$

where \mathbf{x}_1 , \mathbf{x}_2 , \mathbf{u} , and \mathbf{y} are, in general, vectors. Here \mathbf{x}_1 denotes the system states that are available from the output \mathbf{y} ; \mathbf{x}_2 denotes the states of the system to be estimated. Comparing the above system (10) with our perspective system (4), it is clear that $\mathbf{u}(t) = 1$. Further, when both y_1 and y_2 are available in (4), \mathbf{x}_1 and \mathbf{x}_2 in (10) are 2×1 and 1×1 vectors, respectively. When either y_1 or y_2 is available in (4), \mathbf{x}_1 and \mathbf{x}_2 in (10) become 1×1 and 2×1 , respectively. The matrix $w^T(\mathbf{x}_1, \mathbf{u})$ and the vector $g(\mathbf{x}_1, \mathbf{x}_2, \mathbf{u})$ in (10) are, in general, nonlinear functions of their parameters.

An identifier-based observer (IBO) for the system (10) can be designed as

$$\begin{cases} \dot{\hat{\mathbf{x}}}_1 = G A(\mathbf{x}_1 - \hat{\mathbf{x}}_1) + w^T(\mathbf{x}_1, \mathbf{u})\hat{\mathbf{x}}_2 + \phi(\mathbf{x}_1, \mathbf{u}), \\ \dot{\hat{\mathbf{x}}}_2 = -G^2 w(\mathbf{x}_1, \mathbf{u})P(\mathbf{x}_1 - \hat{\mathbf{x}}_1) + g(\mathbf{x}_1, \hat{\mathbf{x}}_2, \mathbf{u}), \\ \hat{\mathbf{x}}(t_i^+) = M \frac{\hat{\mathbf{x}}(t_i^-)}{\|\hat{\mathbf{x}}(t_i^-)\|}, \end{cases} \quad (11)$$

where the sequence of t_i is defined via

$$t_i = \min \{t : t > t_{i-1} \text{ and } \|\hat{\mathbf{x}}(t)\| \geq \gamma M\}, \quad (12)$$

and the matrix P is a positive definite solution of the Lyapunov equation $A^T P + P A = -Q$. In (12), M is an assumed upper bound for the state estimate $\|\hat{\mathbf{x}}(t)\|$, and γ is a fixed constant. The quantity G in (11) is a constant scalar gain. From (11) and (12), the states of the observer are kept bounded, i.e., $\|\hat{\mathbf{x}}(t)\| \leq \gamma M$, where γ is a constant with $\gamma > 1$. Notice that the matrix A in (11) is not the 3×3 parameter matrix in (1).

The assumptions of the IBO include (Jankovic and Ghosh, 1995) the following:

Assumption 1. Assumptions of the IBO:

- $\mathbf{x}(t)$ are bounded. That is, there exists a constant $M > 0$ such that $\|\mathbf{x}(t)\| < M$ for every $t > 0$. Denote by Ω the set $\Omega = \{\mathbf{x} \in \mathbb{R}^n : \|\mathbf{x}(t)\| < M\}$. For a fixed constant $\gamma > 1$, write $\Omega_\gamma = \{\mathbf{x} \in \mathbb{R}^n : \|\mathbf{x}(t)\| < \gamma M\}$.

- The function $g(\mathbf{x}_1, \mathbf{x}_2, \mathbf{u})$ satisfies the following local Lipschitz condition in Ω_γ with respect to \mathbf{x}_2 (Khalil, 2002):

$$\|g(\mathbf{x}_1, \mathbf{x}_2, \mathbf{u}) - g(\mathbf{x}_1, \mathbf{z}_2, \mathbf{u})\| < \alpha_0 \|\mathbf{x}_2 - \mathbf{z}_2\|, \quad (13)$$

where α_0 is a positive constant.

- The matrix $w(\mathbf{x}, \mathbf{u})$ is piecewise smooth, uniformly bounded together with its first time derivative, and there exist positive constants β and ρ such that we have

$$\int_t^{t+\rho} w(\tau)^T w(\tau) d\tau \geq \beta. \quad (14)$$

This assumption is an observability assumption. It resembles the persistence-of-excitation condition, but is stronger.

The three assumptions in Assumption 1 are strict yet reasonable assumptions, referring to the practical system for estimating the 3D states of a point from the observations of its perspective projections. The first two assumptions are standard ones in the control area that guarantee the local existence and uniqueness of a state equation (Khalil, 2002). For the third assumption, we shall later see that, for the case of using both y_1 and y_2 to estimate y_3 , (14) is equivalent to $(b_1 - b_3 y_1)^2 + (b_2 - b_3 y_2)^2 > \varepsilon^2$ for some $\varepsilon > 0$. For $\varepsilon \neq 0$, the above expression defines the complement of a circle on the screen of the camera with the center at $(b_1/b_3, b_2/b_3)$ and radius ε/b_3 . The point $(b_1/b_3, b_2/b_3)$ is called the focus of expression (FOE). It is a well-known fact that the range of a feature point at the FOE cannot be determined. Thus, the above sufficient condition for observability is also necessary for practical purposes (Jankovic and Ghosh, 1995). The first assumption requires the 3D point not to become infinitely close to the center of projection of the camera due to the issue of the FOE. The second assumption requires the 3D point, and also its 2D projection on the imaging surface of the camera, to follow a unique trajectory for a certain initial state and a certain set of affine motion parameters.

Define

$$e_1 = y_1 - \hat{y}_1, \quad e_2 = y_2 - \hat{y}_2, \quad e_3 = y_3 - \hat{y}_3.$$

The constructed IBO observers for the cases when $(y_1(t), y_2(t))$ are available and when only $y_1(t)$ is available, take the following forms (Ma et al., 2004; Ma, 2004):

$$\text{IBO}_{y_1+y_2} : \begin{cases} \begin{bmatrix} \dot{\hat{y}}_1 \\ \dot{\hat{y}}_2 \end{bmatrix} = GA \begin{bmatrix} e_1 \\ e_2 \end{bmatrix} + \begin{bmatrix} b_1 - b_3 y_1 \\ b_2 - b_3 y_2 \end{bmatrix} \hat{y}_3 \\ \quad + \begin{bmatrix} a_{13} + (a_{11} - a_{33})y_1 + a_{12}y_2 \\ a_{23} + a_{21}y_1 + (a_{22} - a_{33})y_2 \end{bmatrix} \\ \quad - \begin{bmatrix} a_{31}y_1^2 + a_{32}y_1y_2 \\ a_{31}y_1y_2 + a_{32}y_2^2 \end{bmatrix}, \\ \dot{\hat{y}}_3 = -G^2 \begin{bmatrix} b_1 - b_3 y_1 & b_2 - b_3 y_2 \end{bmatrix} \\ \quad \times P \begin{bmatrix} e_1 \\ e_2 \end{bmatrix} - (a_{31}y_1 + a_{32}y_2 + a_{33}) \\ \quad \times \hat{y}_3 - b_3 \hat{y}_3^2, \\ \hat{y}(t_i^+) = M \frac{\hat{y}(t_i^-)}{\|\hat{y}(t_i^-)\|}, \end{cases} \quad (15)$$

and

$$\text{IBO}_{y_1} : \begin{cases} \dot{\hat{y}}_1 = GA e_1 + [a_{12} - a_{32}y_1, b_1 - b_3 y_1] \\ \quad \times \begin{bmatrix} \hat{y}_2 \\ \hat{y}_3 \end{bmatrix} + [a_{13} + (a_{11} - a_{33})y_1 - a_{31}y_1^2], \\ \begin{bmatrix} \dot{\hat{y}}_2 \\ \dot{\hat{y}}_3 \end{bmatrix} = -G^2 \begin{bmatrix} a_{12} - a_{32}y_1 \\ b_1 - b_3 y_1 \end{bmatrix} P e_1 \\ \quad + \begin{bmatrix} \tilde{\alpha} \\ -(a_{31}y_1 + a_{32}\hat{y}_2 + a_{33})\hat{y}_3 - b_3 \hat{y}_3^2 \end{bmatrix}, \\ \hat{y}(t_i^+) = M \frac{\hat{y}(t_i^-)}{\|\hat{y}(t_i^-)\|}, \end{cases} \quad (16)$$

where

$$\tilde{\alpha} = a_{23} + a_{21}y_1 + (a_{22} - a_{33})\hat{y}_2 - a_{31}y_1\hat{y}_2 \\ - a_{32}\hat{y}_2^2 + (b_2 - b_3\hat{y}_2)\hat{y}_3,$$

under the corresponding observability conditions

$$\lambda_{\min}\{w([y_1(t), y_2(t)]^T) w^T([y_1(t), y_2(t)]^T)\} > \varepsilon > 0, \quad (17)$$

and

$$\lambda_{\min}\{w(y_1(t)) w^T(y_1(t))\} > \varepsilon > 0, \quad (18)$$

where λ_{\min} denotes the smallest eigenvalue of a matrix.² The sequence of t_i is defined in (12). From (15) and (16), it can be observed that the states of the observers are kept bounded.

² The variable λ has been used extensively in this paper in different places. Here, λ denotes an eigenvalue selector. In Eqns. (21) and (23), λ_i ($i = 1, 2$) denote design parameters. Besides, in (24), λ denotes the design parameter in general.

The two observability conditions in (17) and (18) are of the same complexity. Specifically, they are

$$(b_1 - b_3 y_1)^2 + (b_2 - b_3 y_2)^2 > 0, \\ \lambda_{\min} \left\{ \begin{bmatrix} \bar{a}^2 & \bar{a}\bar{b} \\ \bar{a}\bar{b} & \bar{b}^2 \end{bmatrix} \right\} > 0, \quad (19)$$

with $\bar{a} = a_{12} - a_{32}y_1$ and $\bar{b} = b_1 - b_3y_1$. The above two conditions are equivalent to

$$(b_1 - b_3 y_1)^2 + (b_2 - b_3 y_2)^2 > 0, \\ (b_1 - b_3 y_1)^2 + (a_{12} - a_{32} y_1)^2 > 0. \quad (20)$$

A detailed proof of the IBO in the general form was provided in (Jankovic and Ghosh, 1995). For the readability of the paper, a sketched proof of the IBO is given in Appendix. The proof of the IBO is not our main contribution.

3.2. Direct Modification of the SMO

The following SMO observer proposed in (Chen and Kano, 2002) has been applied to the state estimation of (4) when both $y_1(t)$ and $y_2(t)$ are available under Assumption 1:

$$\text{SMO}_{y_1+y_2} : \left\{ \begin{array}{l} \begin{bmatrix} \dot{\hat{y}}_1 \\ \dot{\hat{y}}_2 \end{bmatrix} = \begin{bmatrix} \frac{\hat{\lambda}_1(t)e_1}{|e_1| + \delta_1} \\ \frac{\hat{\lambda}_2(t)e_2}{|e_2| + \delta_2} \end{bmatrix} + \begin{bmatrix} b_1 - b_3 y_1 \\ b_2 - b_3 y_2 \end{bmatrix} \\ \quad \times \hat{y}_3 + \begin{bmatrix} a_{13} + (a_{11} - a_{33})y_1 + a_{12}y_2 \\ a_{23} + a_{21}y_1 + (a_{22} - a_{33})y_2 \\ - \begin{bmatrix} a_{31}y_1^2 + a_{32}y_1y_2 \\ a_{31}y_1y_2 + a_{32}y_2^2 \end{bmatrix} \end{bmatrix}, \\ \dot{\hat{y}}_3 = \alpha [b_1 - b_3 y_1, b_2 - b_3 y_2] \begin{bmatrix} \frac{\hat{\lambda}_1(t)e_1}{|e_1| + \delta_1} \\ \frac{\hat{\lambda}_2(t)e_2}{|e_2| + \delta_2} \end{bmatrix} \\ \quad - (a_{31}y_1 + a_{32}y_2 + a_{33})\hat{y}_3 - b_3\hat{y}_3^2, \\ \hat{y}(t_i^+) = M \frac{\hat{y}(t_i^-)}{\|\hat{y}(t_i^-)\|}, \end{array} \right. \quad (21)$$

where δ_i ($i = 1, 2$) are design parameters. Here $\hat{\lambda}_i(t)$ ($i = 1, 2$) are adaptively updated by

$$\dot{\hat{\lambda}}_1(t) = \begin{cases} 2\alpha_1 |e_1|, & \text{if } |e_1| > 2\delta_1, \\ 0, & \text{otherwise,} \end{cases} \\ \dot{\hat{\lambda}}_2(t) = \begin{cases} 2\alpha_2 |e_2|, & \text{if } |e_2| > 2\delta_2, \\ 0, & \text{otherwise,} \end{cases} \quad (22)$$

where α , α_1 , and α_2 are positive constants and δ_i for $i = 1, 2$ are design parameters. Furthermore, $\hat{\lambda}_1(0)$ and $\hat{\lambda}_2(0)$ can be any positive constants.

When only $y_1(t)$ is available, the following observer, which is based on a modification of the SMO and a resemblance between the SMO and the IBO, can also be used for the state estimation of $y_2(t)$ and $y_3(t)$:

$$\text{SMO}_{y_1} : \left\{ \begin{array}{l} \dot{\hat{y}}_1 = \frac{\hat{\lambda}_1(t)e_1}{|e_1| + \delta_1} + [a_{12} - a_{32}y_1, b_1 - b_3y_1] \\ \quad \times \begin{bmatrix} \hat{y}_2 \\ \hat{y}_3 \end{bmatrix} + [a_{13} + (a_{11} - a_{33})y_1 - a_{31}y_1^2], \\ \begin{bmatrix} \dot{\hat{y}}_2 \\ \dot{\hat{y}}_3 \end{bmatrix} = \alpha \begin{bmatrix} a_{12} - a_{32}y_1 \\ b_1 - b_3y_1 \end{bmatrix} \frac{\hat{\lambda}_1(t)e_1}{|e_1| + \delta_1} \\ \quad + \begin{bmatrix} \tilde{\alpha} \\ -(a_{31}y_1 + a_{32}\hat{y}_2 + a_{33})\hat{y}_3 - b_3\hat{y}_3^2 \end{bmatrix}, \\ \hat{y}(t_i^+) = M \frac{\hat{y}(t_i^-)}{\|\hat{y}(t_i^-)\|}, \end{array} \right. \quad (23)$$

where

$$\tilde{\alpha} = a_{23} + a_{21}y_1 + (a_{22} - a_{33})\hat{y}_2 - a_{31}y_1\hat{y}_2 \\ - a_{32}\hat{y}_2^2 + (b_2 - b_3\hat{y}_2)\hat{y}_3.$$

The sequence of t_i in (21) and (23) is similar to that defined in (12). Again, the states of the observers (21) and (23) are kept bounded. The modified SMO observer SMO_{y_1} in (23) achieves an extremely similar performance to IBO using properly chosen observer parameters, as will be seen in Section 4.

The original SMO observer is designed to estimate $y_3(t)$ using $y_1(t)$ and $y_2(t)$, and its proof was focused on the specific system (4) instead of the more general nonlinear systems in (10). In the following, an alternative proof of the SMO for the nonlinear system (10) is provided.

3.3. Extended Proof of the SMO

In this section, we provide an alternative proof of the SMO for nonlinear systems in the form of (10) under Assumption 1. First, consider the following error dynamics:

$$\begin{cases} \dot{e}_1 = -\lambda \text{sgn}(e_1) + w^T(x_1, \mathbf{u})e_2, \\ \dot{e}_2 = -\alpha \lambda w(x_1, \mathbf{u}) \text{sgn}(e_1) \\ \quad + g(x_1, x_2, \mathbf{u}) - g(x_1, \hat{x}_2, \mathbf{u}), \end{cases} \quad (24)$$

with $e_1 = \mathbf{x}_1 - \hat{\mathbf{x}}_1$, $e_2 = \mathbf{x}_2 - \hat{\mathbf{x}}_2$ and $\text{sgn}(\cdot)$ giving the sign of its argument.³ Assume now that⁴

$$g(\mathbf{x}_1, \mathbf{x}_2, \mathbf{u}) - g(\mathbf{x}_1, \hat{\mathbf{x}}_2, \mathbf{u}) = 0. \quad (25)$$

The system (24) becomes

$$\begin{cases} \dot{e}_1 = -\lambda \text{sgn}(e_1) + w^T(\mathbf{x}_1, \mathbf{u})e_2, \\ \dot{e}_2 = -\alpha \lambda w(\mathbf{x}_1, \mathbf{u}) \text{sgn}(e_1). \end{cases} \quad (26)$$

First, it can be shown that e_1, e_2 and \dot{e}_1 are bounded. For example, $e_1 = \mathbf{x}_1 - \hat{\mathbf{x}}_1$ is bounded due to the boundedness of the state estimate \mathbf{x}_1 (by assumption) and $\hat{\mathbf{x}}_1$. The boundedness of $\hat{\mathbf{x}}_1$ can be seen from the third equation in (21) and (23), where the states of the observers are kept bounded. Similarly, e_2 is bounded. Then, from (24), \dot{e}_1 is bounded due to the boundedness of e_1, e_2 and $w^T(\mathbf{x}, \mathbf{u})$ (by the third proviso in Assumption 1).

Let $V_1 = \frac{1}{2}(e_1^2 + e_2^2)$. Then

$$\begin{aligned} \dot{V}_1 &= e_1^T \dot{e}_1 + e_2^T \dot{e}_2 \\ &= -e_1^T \lambda \text{sgn}(e_1) + e_1^T w^T e_2 - \alpha e_2^T \lambda w \text{sgn}(e_1) \\ &= -\lambda \|e_1^T\| + e_2^T w (e_1 + \alpha(\dot{e}_1 - w^T e_2)) \\ &= -\lambda \|e_1^T\| - \alpha \|w^T e_2\|^2 + e_2^T w (e_1 + \alpha \dot{e}_1). \end{aligned} \quad (27)$$

Since e_1, \dot{e}_1, e_2 , and w are bounded, $e_2^T w (e_1 + \alpha \dot{e}_1)$ are bounded. By choosing α and λ large enough, \dot{V}_1 can be made

$$\dot{V}_1 \leq -\bar{\lambda} \|e_1\|^2 - \bar{\alpha} \|w^T e_2\|^2 \leq 0, \quad (28)$$

where $\bar{\lambda}$ and $\bar{\alpha}$ are two constants different from λ and α , respectively. The selection of the design parameter λ is dependent on the initial condition of the system. It should be significantly larger than a function of the initial condition of the system. Further, because of (14), we can

³ More precisely, $\text{sgn}(e_1)$ should be understood as $[\text{sgn}(e_1), \text{sgn}(e_2), \dots, \text{sgn}(e_m)]^T$ assuming that the vector e_1 is an $m \times 1$ vector. That is, $e_1 = [e_1, e_2, \dots, e_m]^T$.

⁴ This assumption will be relieved later when deriving (31).

have

$$\begin{aligned} \int_t^{t+\delta} \dot{V}_1 d\tau &\leq - \left[\bar{\lambda} \int_t^{t+\delta} \|e_1(\tau)\|^2 d\tau \right. \\ &\quad \left. + \bar{\alpha} \int_t^{t+\delta} \|w^T(\tau)e_2(\tau)\|^2 d\tau \right] \\ &\leq - \left[\bar{\lambda} \int_t^{t+\delta} \|e_1(\tau)\|^2 d\tau \right. \\ &\quad \left. + \bar{\alpha} \beta \int_t^{t+\delta} \|e_2(\tau)\|^2 d\tau \right] \\ &= -(\bar{\lambda} e_1^2 + \bar{\alpha} \beta e_2^2) \leq -\tilde{\lambda} V_1, \end{aligned} \quad (29)$$

where $\tilde{\lambda} = \min(\bar{\lambda}, \bar{\alpha}\beta)$. According to Theorem 4.5 in (Khalil, 2002), the system (26) is exponentially stable due to (28) and (29).

Now, consider Eqn. (24). Following the converse theorem (Khalil, 2002), there exists another Lyapunov function V_2 and four positive constants c_i for $i = 1, 2, 3, 4$ such that

$$\begin{aligned} c_1 \|e\|^2 &< V_2 < c_2 \|e\|^2, \quad \dot{V}_2|_{(26)} < -c_3 \|e\|^2, \\ \left\| \frac{\partial V_2}{\partial e} \right\| &< c_4 \|e\|, \end{aligned} \quad (30)$$

where $e = [e_1^T, e_2^T]^T$, and $\dot{V}_2|_{(26)}$ denotes the time derivative of V_2 calculated along the trajectory of the system (26). Discarding the assumption of $g(\mathbf{x}_1, \mathbf{x}_2, \mathbf{u}) - g(\mathbf{x}_1, \hat{\mathbf{x}}_2, \mathbf{u}) = 0$ as stated in (25) and using V_2 as the Lyapunov function for the system (24), we can obtain

$$\begin{aligned} \dot{V}_2|_{(24)} &= \frac{d}{dt} V_2|_{(26)} \\ &\quad + \left\| \frac{\partial V_2}{\partial e} \right\| (g(\mathbf{x}_1, \mathbf{x}_2, \mathbf{u}) - g(\mathbf{x}_1, \hat{\mathbf{x}}_2, \mathbf{u})), \quad (31) \\ &\leq -c_3 \|e\|^2 + c_4 \|e\| \alpha_0 \|\mathbf{x}_2 - \hat{\mathbf{x}}_2\| \\ &\leq -(c_3 - c_4 \alpha_0) \|e\|^2, \end{aligned}$$

where the function $g(\mathbf{x}_1, \mathbf{x}_2, \mathbf{u})$ is assumed to satisfy the local Lipschitz condition (13) as stated in Assumption 1. $\dot{V}_2|_{(24)}$ can be made a negative definite function by choosing $c_3 > c_4 \alpha_0$, so that the system (24) becomes exponentially stable.

Replacing $\lambda \text{sgn}(e_1)$ by $\hat{\lambda} \frac{e_1}{\|e_1\| + \delta_1}$ in (24), we arrive at the error dynamics when using the SMO observer. Following the same procedures from Eqns. (24) to (27), in (27), the first element becomes $-\hat{\lambda} e_1^T \frac{e_1}{\|e_1\| + \delta_1}$. Again, by

choosing α and $\hat{\lambda}$ large enough, Eqn. (28) can be made true. The following proof remains the same as those from Eqns. (28) to (31). ■

Remark 1. $\frac{e_1}{|e_1|+\delta_1}$ is introduced to replace $\text{sgn}(e_1)$ to reduce the chattering and the singularity effect because $e(t)$ might be zero. Besides, when $\delta_1 \rightarrow 0$, $\frac{e_1}{|e_1|+\delta_1} \rightarrow \text{sgn}(e_1)$.

3.4. PDS with an Alternative Output Definition

Besides defining $y(t)$ as in (3), we can also let

$$\begin{aligned} y(t) &= [y_1(t), y_2(t), y_3(t)]^T \\ &= [X(t)/Y(t), Z(t)/Y(t), 1/Y(t)]^T. \end{aligned} \quad (32)$$

The derivative of $y(t)$ then becomes

$$\begin{cases} \dot{y}_1 = a_{11}y_1 + a_{12} + a_{13}y_2 \\ \quad - (a_{21}y_1 + a_{22} + a_{23}y_2)y_1 \\ \quad + (b_1 - b_2y_1)y_3, \\ \dot{y}_2 = a_{31}y_1 + a_{32} + a_{33}y_2 \\ \quad - (a_{21}y_1 + a_{22} + a_{23}y_2)y_2 \\ \quad + (b_3 - b_2y_2)y_3, \\ \dot{y}_3 = -(a_{21}y_1 + a_{22} + a_{23}y_2)y_3 - b_2y_3^2. \end{cases} \quad (33)$$

The PDS system in (33) can be understood as the PDS in (4) goes through another perspective projection, which might be called a ‘‘chained perspective projection’’, when only $X(t)/Y(t) = \frac{X(t)/Z(t)}{Y(t)/Z(t)}$ is measurable. In comparison, the PDS in (4) uses the two coordinates of a projected point on the image plane as the measurements, while the chained PDS system in (33) requires only a slope. The system (33) can also be understood as a result from a camera facing towards the Y axis, instead of the Z axis as in (4). Due to this, the resulting PDS in (33) is equivalent to (4) by switching orders of the motion parameters as

$$[a]_{i,j} = \begin{bmatrix} a_{11} & a_{13} & a_{12} \\ a_{31} & a_{33} & a_{32} \\ a_{21} & a_{23} & a_{22} \end{bmatrix}, \quad [b]_j = \begin{bmatrix} b_1 \\ b_3 \\ b_2 \end{bmatrix}. \quad (34)$$

We thus show that, sticking to the perspective projection, different output definitions result in perspective dynamics systems in a similar form. Thus, in Section 4, simulation results for the PDS in (4) are only presented without loss of generality.

4. Simulation Results

The observers IBO and SMO are implemented via Matlab simulations. First, we show an example of simulation results using the first example in (Chen and Kano, 2002), where the target is assumed to move according to the following affine motion:

$$\begin{bmatrix} \dot{X}(t) \\ \dot{Y}(t) \\ \dot{Z}(t) \end{bmatrix} = \begin{bmatrix} -0.2 & 0.4 & -0.6 \\ 0.1 & -0.2 & 0.3 \\ 0.3 & -0.4 & 0.4 \end{bmatrix} \times \begin{bmatrix} X(t) \\ Y(t) \\ Z(t) \end{bmatrix} + \begin{bmatrix} 0.5 \\ 0.25 \\ 0.3 \end{bmatrix},$$

$$(X_0, Y_0, Z_0) = (1, 1.5, 2.5),$$

$$y_0 = (X_0/Z_0, Y_0/Z_0, 1/Z_0). \quad (35)$$

In all the simulations, the output is corrupted with uniform noise bounded by $\pm 10^{-2}$. Here y'_0 is chosen to be $(0, 0, 0)$. The observer parameters are:⁵

- IBO: $G = 10, A = 1, P = -1/2, M = 10, \gamma = 1$.
- SMO: $\alpha = 5, \hat{\lambda}_1(0) = 1, \alpha_1 = 10, \delta_1 = 0.2, M = 10, \gamma = 1$.

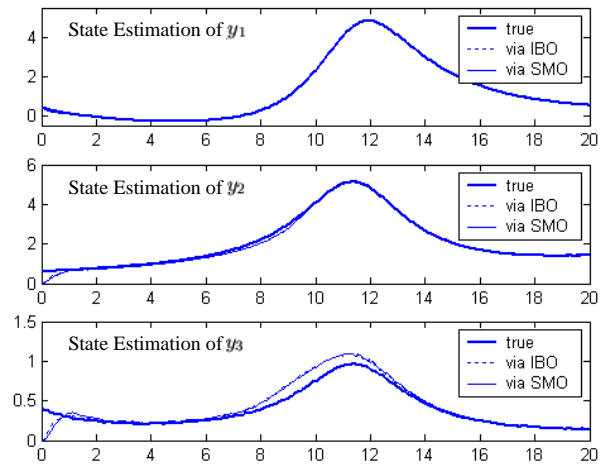


Fig. 3. State estimation of (y_2, y_3) using y_1 for the motion dynamics in (35).

State estimation using only y_1 via IBO and SMO are presented in Fig. 3, where the true state trajectories are plotted in solid lines and the estimates are represented

⁵ For the cases with a single homogeneous function and with both (y_1, y_2) .

by dotted and dashed lines for the IBO and SMO, respectively. It can be observed that the state estimation of (y_2, y_3) can be achieved and the performance of IBO and SMO are extremely close.

Figure 4 shows a comparison between IBO and IBO for y_3 . The simulation time is set to be 80 seconds to clearly show the error convergence. It is obvious that IBO generally outperforms IBO, during the transient period, but both converge to the true value. A simulation comparison between SMO and SMO is not provided due the similar performance of the SMO with the IBO.

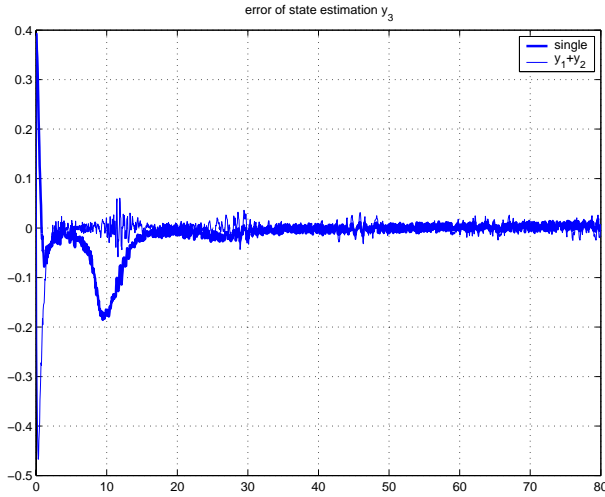


Fig. 4. Estimation error comparison between IBO and IBO for the motion dynamics in (35).

Other examples of simulation results are presented in Figs. 5 and 6 for the following affine motion:

$$\begin{bmatrix} \dot{X}(t) \\ \dot{Y}(t) \\ \dot{Z}(t) \end{bmatrix} = \begin{bmatrix} -0.2 & 0.4 & -0.6 \\ 0.1 & -0.2 & 0.3 \\ -0.4 & 0.4 & -0.4 \end{bmatrix} \times \begin{bmatrix} X(t) \\ Y(t) \\ Z(t) \end{bmatrix} + \begin{bmatrix} 0.5 \\ 0.25 \\ 0.3 \end{bmatrix},$$

$$(X_0, Y_0, Z_0) = (1, 1.5, 2.5),$$

$$y_0 = (X_0/Z_0, Y_0/Z_0, 1/Z_0). \quad (36)$$

Remark 2. Range identification with general 3D planar imaging surfaces: It has been shown in the above simulations that state estimation using y_1 and y_2 generally

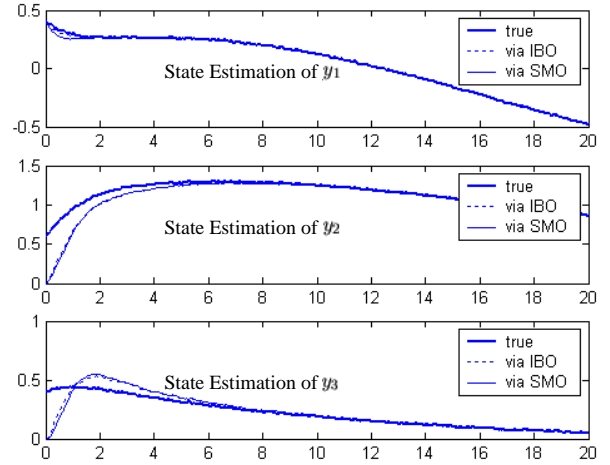


Fig. 5. State estimation of (y_2, y_3) using y_1 for the motion dynamics in (36).

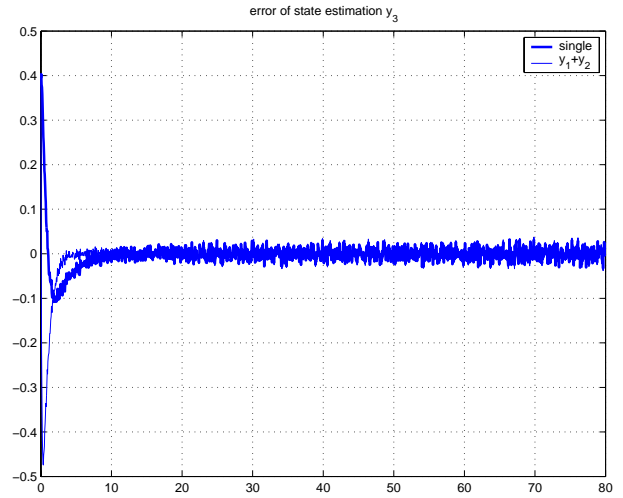


Fig. 6. Estimation error comparison between IBO and IBO for the motion dynamics in (36).

outperforms the situation when using only a single observation. Motivated by these results, it is straightforward to ask: if using full homogeneous observations is “better” (in the sense of the state estimation accuracy) than using partial observations, will a general planar imaging surface as shown in Fig. 1 outperform the traditional camera-type imaging surface ($Z_p = 1$)? We believe that the answer is “yes” intuitively, because when using a general planar imaging surface and considering the nonlinear system in (10), x_1 becomes a 3×1 vector, compared to the 2×1 vector as in the case of $Z_p = 1$. However, it is obvious that this benefit is achieved at the cost of more complex imaging systems.

5. Concluding Remarks

For a perspective dynamic system (PDS) with a single homogeneous observation function, the range identification problem is discussed using nonlinear observers previously used for the full observation case. Our simulation results show that the convergence speed of the observer for the single observation case is slower than those with full observations. However, both the observers have similar performance. This study also shows that a more general 3D imaging surface can be more desirable since it can provide more homogeneous output(s).

The sensitivity of the state estimation of a PDS with respect to motion parameters is not investigated in this paper. However, it would not be surprising that the effect can be slightly more severe for the single case than that with full observations.

References

- Chen X. and Kano H. (2002): *A new state observer for perspective systems*. — IEEE Trans. Automat. Contr., Vol. 47, No. 4, pp. 658–663.
- Chiuso A., Favaro P., Jin H. and Soatto S. (2002): *Structure from motion causally integrated over time*. — IEEE Trans. Pattern Anal. Mach. Intell., Vol. 24, No. 4, pp. 523–535.
- Cho H.R., Lee K.M. and Lee S.U. (2001): *A new robust 3D motion estimation under perspective projection*. — Proc. IEEE Int. Conf. Image Processing, Thessaloniki, Greece, pp. 660–663.
- Dixon W.E., Fang Y., Dawson D.M. and Flynn T.J. (2003): *Range identification for perspective vision systems*. — IEEE Trans. Automat. Contr., Vol. 48, No. 12, pp. 2232–2238.
- Ghosh B.K., Jankovic M. and Wu Y.T. (1994): *Perspective problems in system theory and its application to machine vision*. — J. Math. Syst. Estim. Contr., Vol. 4, No. 1, pp. 3–38.
- Hernandez C.N., Banks S.P. and Aldeen M. (2003): *Observer design for nonlinear systems using linear approximations*. — IMA J. Math. Contr. Inf., Vol. 20, pp. 359–370.
- Jankovic M. and Ghosh B.K. (1995): *Visually guided ranging from observations of points, lines and curves via an identifier based nonlinear observer*. — Syst. Contr. Lett., Vol. 25, pp. 63–73.
- Khalil H.K. (2002): *Nonlinear Systems*. — New Jersey: Prentice Hall.
- Ma L. (2004): *Vision-Based Measurements for Dynamic Systems and Control*. — Ph.D. thesis, Utah State University.
- Ma L., Chen Y. and Moore K.L. (2004): *Range identification for perspective dynamic system with single homogeneous observation*. — Proc. IEEE Int. Conf. Robot. and Automat., New Orleans, pp. 5207–5211.
- Morgan A.P. and Narendra K.S. (1977): *On the stability of nonautonomous differential equations $\dot{x} = (A + B(t))x$ with skew symmetric matrix $B(t)$* . — SIAM J. Contr., Vol. 15, No. 1, pp. 163–176.
- Papadimitriou T., Diamantaras K.I., Stryntz M.G. and Roumeliotis M. (2000): *Robust estimation of rigid-body 3-D motion parameters based on point correspondences*. — IEEE Trans. Circ. Syst. Video Technol., Vol. 10, No. 4, pp. 541–549.
- Soatto S., Frezza R. and Perona P. (1996): *Motion estimation via dynamic vision*. — IEEE Trans. Automat. Contr., Vol. 41, No. 3, pp. 393–413.
- Tomas-Rodriguez M. and Banks S.P. (2003): *Linear approximations to nonlinear dynamical systems with applications to stability and spectral theory*. — IMA J. Math. Contr. Inf., Vol. 20, pp. 89–103.

Appendix

Sketched Proof of the IBO (Jankovic and Ghosh, 1995)

Consider the following differential equation for the estimation error from (10) and (11):

$$\dot{e}_1 = GAe_1 + w^T(x_1, u)e_2,$$

$$\dot{e}_2 = -G^2w(x_1, u)Pe_1 + g(x_1, x_2, u) - g(x_1, \hat{x}_2, u).$$

Define a linear change of the coordinates $\xi = Te$ via

$$T = \begin{bmatrix} G^{-1}I_{n_1} & 0 \\ 0 & G^{-2}I_{n_2} \end{bmatrix},$$

where n_1 and n_2 correspond to the dimensions of x_1 and x_2 , respectively. It can be verified that the error dynamics in the new state ξ can be written in the following form:

$$\dot{\xi}_1 = G(A\xi_1 + w^T(t)\xi_2), \quad (37)$$

$$\dot{\xi}_2 = Gw(t)P\xi_1 + G^{-2}(g(x_1, x_2, u) - g(x_1, \hat{x}_2, u)),$$

where $w(t)$ is considered a function of time since $x_1(t)$ and $u(t)$ are fixed functions of time known at every time instant. Assume that $g(x_1, x_2, u) - g(x_1, \hat{x}_2, u) = 0$, and define the new time coordinate via $s = Gt$. The differential equation (37) becomes

$$\frac{d\xi_1}{ds} = A\xi_1 + \bar{w}^T(s)\xi_2, \quad \frac{d\xi_2}{ds} = \bar{w}(s)P\xi_1, \quad (38)$$

where $\bar{w}(s) = w(G^{-1}s)$. The above system is in the form satisfied by the error differential equation in the parameter identification problem considered in (Morgan and Narendra, 1977), and it can be shown that the above system is

exponentially stable from Assumption 1. For the system given by (38), it can be verified that the proof of Theorem 2 in (Morgan and Narendra, 1977) guarantees the existence of a Lyapunov function $V_1(\xi)$ and three positive constants $d_i, i = 1, 2, 3$ such that

$$d_1 \|\xi(s)\|^2 < V_1(\xi) < d_2 \|\xi(s)\|^2,$$

$$\frac{d}{ds} V_1(\xi)|_{(38)} \leq 0,$$

$$\int_s^{s+\rho} \frac{d}{d\tau} V_1(\xi)|_{(38)} d\tau \leq -d_3 \|\xi(s)\|^2,$$

where $\dot{V}_1(\xi)|_{(38)}$ means that the time derivative of V_1 is calculated along the trajectory of the system (38). Following the converse theorem in (Khalil, 2002), there exist another Lyapunov function $V_2(\xi, s)$ and four positive constants $c_i, i = 1, 2, 3, 4$ such that

$$c_1 \|\xi(s)\|^2 < V_2(\xi, s) < c_2 \|\xi(s)\|^2,$$

$$\dot{V}_2(\xi, s)|_{(38)} < -c_3 \|\xi(s)\|^2,$$

$$\left\| \frac{\partial V_2(\xi, s)}{\partial \xi} \right\| < c_4 \|\xi(s)\|. \quad (39)$$

Discarding the assumption that $g(x_1, x_2, \mathbf{u}) - g(x_1, \hat{x}_2, \mathbf{u}) = 0$, the error dynamics in ξ and s is given by

$$\frac{d\xi_1}{ds} = A\xi_1 + \bar{w}^T(s)\xi_2, \quad (40)$$

$$\frac{d\xi_2}{ds} = \bar{w}(s)P\xi_1 + G^{-3}(g(x_1, x_2, \mathbf{u}) - g(x_1, \hat{x}_2, \mathbf{u})).$$

Using the function $V_2(\xi, s)$ as the Lyapunov candidate for the above system, we can obtain

$$\frac{d}{ds} V_2(\xi, s)|_{(40)} \leq (-c_3 + G^{-1}c_4\alpha_0) \|\xi\|^2.$$

It is obvious that $\dot{V}_2(\xi, s)|_{(40)}$ can be made a negative definite function by choosing $G > c_4\alpha_0/c_3$. For such a choice of G , the system (40) becomes exponentially stable. Because the linear relationship between ξ and e , it can be concluded that e converges to zero exponentially between discontinuities.

Received: 23 August 2004

Revised: 10 November 2004

Re-revised: 10 January 2005